A TERRAIN–FOLLOWING BOUSSINESQ SYSTEM*

ANDRÉ NACHBIN†

Abstract. A long wave model is derived asymptotically from the nonlinear potential theory equations. The flow regime of interest is incompressible, irrotational and inviscid. Asymptotic analysis leads to a weakly nonlinear, weakly dispersive (variable coefficient) Boussinesq system valid for a wide class of topographies. The mild slope hypothesis is not required and rapidly varying topographies are also considered. In analogy with atmospheric models we use a terrain-following coordinate system. The novelty being that this coordinate system naturally suggests the weighted averaging of terrain-following velocity components, as opposed to the depth-average of horizontal velocity components found in standard shallow water formulations. Furthermore, a Schwarz-Christoffel Toolbox is used to provide additional insight on these new results. Regarding applications the proposed model can be used for studying solitary waves interacting with fine scale inhomogeneities, a theme of great interest. The terrain-following model also presents potential numerical advantages for Boussinesq solvers.

Key words. dispersive waves, inhomogeneous media, asymptotic theory

AMS subject classifications. 76B07, 76B15, 35Q

1. Introduction.

Shallow water (long wave) models have been known and studied for many years. Among several important partial differential equations that fall into this class are weakly dispersive, weakly nonlinear models such as the Korteweg-de Vries (KdV) equation or the Boussinesq equations [7, 16]. The flow regime considered is incompressible, irrotational and inviscid. These long wave models can be derived asymptotically from the nonlinear potential theory equations when the leading order terms, in the nonlinearity and dispersion parameters, are retained. Their analysis has received a great deal of attention from both the mathematical theory and applications viewpoints.

Of great research interest are problems involving these models in the presence of heterogeneous media, which can be of different nature depending on the application. Shallow water models are not only of interest in ocean applications but also very commom in meteorology [5], where the shallow propagation medium is the atmosphere. Literature is abundant on the mathematical analysis of long wave models, their numerical discretization and behaviour, as well as the implementation of oceanic and atmospheric simulators. Reference to some of this work will not be attempted due to the richness of the subject. It is bound to be injudicious.

This work is concerned with the derivation of a long wave model valid in the presence of a wide class of bottom profiles, including rapidly varying topographies. Most of the well established long wave models are derived under the hypothesis of having mild slope topographies. Among others, we mention three interesting recent work which improve classical shallow water models and include topographic effects. Camassa, Holm and Levermore [2] derive shallow water equations that have a Hamiltonian principle formulation and which model long-time effects of slowly varying topographies. Milewski [8] considers the propagation of long waves on the surface of a three-dimensional fluid domain bounded below by a slowly varying topography. Weakly nonlinear wave-topography interaction is studied in two limits giving rise to a vari-

*This work was supported by CNPq/Brazil under Grant 300368/96-8 and NEC/CEMAT–IMPA under Grant DMS 2.419/98-00.

†Instituto de Matemática Pura e Aplicada, Est. D. Castorina 110, Jardim Botânico, Rio de Janeiro, RJ 22460-320, Brazil (nachbin@impa.br).

able coefficient KdV equation or a variable coefficient KP (Kadomtsev-Petviashvili) equation. We also mention the work of Schäffer and Madsen [15] who derive a new set of Boussinesq equations which provide improvements for the linear dispersion relation and shoaling characteristics. For rapidly varying topographies it is worth mentioning the earlier work of Rosales and Papanicolaou [14] where effective KdV equations were derived for rapidly varying periodic and (small amplitude) random topographies. But in both cases back-scattering is negligible. Finally we point out the work of Hamilton [6] which is the starting point for the present paper. Hamilton used a conformal mapping technique to derive long wave models on a fluid of rapidly varying depth. In particular a Boussinesq system is presented ([6] (A14-A15)) in the form of a second order in time 2x2 system. The dependent variables considered are the depth-averaged potential and wave elevation. We derive a first order 2x2 Boussinesq system in terms of the wave elevation and the averaged terrain-following velocity components. For flat channels our system reduces to the standard Boussinesq system found in the literature [7, 16]. Hamilton's conformal mapping technique has also been used by the author to study the reflection-transmission problem over disordered (random) topographies [11, 12, 13].

Moreover our main result is the derivation of a weakly nonlinear, weakly dispersive (variable coefficient) Boussinesq system valid for a wide class of topographies and multiple scattering problems. The mild slope hypothesis is not required. In analogy with some atmospheric models [3] we use a terrain-following coordinate system for the independent variables. This curvilinear coordinate system is obtained from the theory of conformal mappings as suggested in Hamilton [6]. Hamilton does not use dimensionless variables and performs the asymptotic simplification of equations arguing through chosen length scales. As mentioned above his formulation of a nonlinear Boussinesq system is briefly outlined in Appendix A [6]. Our approach is to perform the asymptotic simplification of the nonlinear potential theory equations in a systematic way (as in Whitham [16]) by using dimensionless variables and the conformal mapping setting of Hamilton. All steps in the derivation are presented. The curvilinear coordinate system naturally suggests the weighted averaging of terrain-following velocity components, as opposed to the depth-average of horizontal components found in standard shallow water formulations. For rapidly varying topographies the standard depth-average strategy breaks down. As pointed out by Hamilton [6] the truncation term in the near-bottom series expansion will dominate the leading order terms when the bottom is rapidly varying (top of page 292 [6]). In the dimensionless formulation (given below in section 2) the large truncation term will be caused by the β/γ term in the Neumann condition, when γ is small. In contrast the asymptotic expansion, for the free surface conditions in the curvilinear coordinates, generates truncation terms that are negligible compared to the leading order ones. The Neumann condition is trivial in this framework as will be shown in section 4.

Furthermore, our use of dimensionless variables enables a better understanding of the impact of the conformal mapping technique on the asymptotic analysis. Using Driscoll's [4] MATLAB Schwarz-Christoffel Toolbox we provide additional insight on why the terrain-following Boussinesq system is a good model even in the presence of rapidly varying topographies. Using the SC-Toolbox we graph the curvilinear coordinate system for both slowly and rapidly varying topographies. The average of terrain-following velocity components is clearly seen as a weighted average along special curves, orthogonal to the topography and to the undisturbed free surface. This weighted averaging naturally adjusts to either slowly varying or rapidly varying topographies, as will be shown graphically with the SC-Toolbox.

Another result of interest is that the nonlinear shallow water equations can be viewed as an $O(\alpha, \sqrt{\beta})$ approximation of the full potential theory equations. The standard notation is used: α is the nonlinearity parameter and β the dispersion parameter. The nonlinear shallow water system is (of course) hyperbolic, but the square root of the dispersion parameter plays a role only on the smoothing of sharp features of the topography. This had been pointed out by Hamilton [6], but the rate of smoothing was not explicitly identified, nor the nonlinear shallow water equation presented.

The proposed model can be used for studying solitary waves over disordered (random) topographies, a theme of great interest [9, 10]. This could not have been done with existing Boussinesq models. We are currently investigating the numerical advantages of working with this model. A potential advantage resides on the fact that within this new framework, the variable ("topographic") coefficient moves away from the dispersive term (a third order derivative) and places itself at first order terms. We have results that indicate the improved performance of our Boussinesq solvers [10].

The paper is organized as follows. In section 2 we present the standard scaling [16] and the (dimensionless) nonlinear potential theory equations in cartesian coordinates. Section 3 describes the conformal mapping theory in full detail along with the calculation of the variable free surface coefficient's leading order term. The (dimensionless) nonlinear potential theory equations, in curvilinear coordinates, are presented in section 4 and the weakly nonlinear, weakly dispersive asymptotic theory in section 5. The applications and conclusions are given in section 6. Appendix A contrasts the terrain-following Boussinesq system with standard Boussinesq formulations.

2. Formulation and scaling. Let variables with physical dimensions be denoted with a tilde. We introduce the length scales σ (a typical pulse width or wavelength), h_0 (a typical depth), a (a typical wave amplitude), l_b (the horizontal length scale for bottom irregularities) and L (the total length of the rough region or the total propagation distance). The acceleration due to gravity is denoted by g and the reference shallow water speed is $c_0 = \sqrt{gh_0}$. Dimensionless variables are then defined in a standard fashion [14, 16] by having

$$\tilde{x} = \sigma x \qquad \tilde{y} = h_0\, y \qquad \tilde{t} = \left(\frac{\sigma}{c_0}\right) t$$

$$\tilde{\eta} = a\,\eta \qquad \tilde{\phi} = \left(\frac{g\sigma a}{c_0}\right)\phi \qquad \tilde{h} = h_0\, H\left(\frac{\tilde{x}}{l_b}\right).$$

The velocity potential $\phi(x,y,t)$ and wave elevation $\eta(x,t)$ satisfy the dimensionless equations [16]:

$$\beta\,\phi_{xx} + \phi_{yy} = 0 \quad \text{for} \quad -H(x/\gamma) < y < \alpha\eta(x,t),$$

with the nonlinear free surface conditions

$$\eta_t + \alpha\phi_x\eta_x - \frac{1}{\beta}\phi_y = 0$$

$$\eta + \phi_t + \frac{\alpha}{2}\left(\phi_x^2 + \frac{1}{\beta}\phi_y^2\right) = 0$$

at $y = \alpha\eta(x,t)$. The Neumann condition at the impermeable bottom is

$$\phi_y + \frac{\beta}{\gamma}\, H'(x/\gamma)\phi_x = 0.$$

The bottom topography is described by $y = -H(x/\gamma)$ where

$$H(x/\gamma) \quad = \quad \begin{cases} 1 + n(x/\gamma) & \text{when } \; 0 < x < L \\ 1 & \text{when } \; x \le 0 \; \text{ or } \; x \ge L. \end{cases}$$

The bottom profile is described by the (possibly rapidly varying) function $-n(x/\gamma)$. The topography is rapidly varying when $\gamma \ll 1$. The undisturbed depth is given by $y = \quad -1$ and the topography can be of large amplitude provided that $|n| < 1$. We do not need to assume that the fluctuations n are small, nor continuous, nor slowly varying.

The following dimensionless parameters arise:

$\alpha = a/h_0$ (nonlinearity parameter)

$\beta = h_0^2/\sigma^2$ (dispersion parameter)

$\gamma = l_b/\sigma$ (bottom irregularities compared to the wavescale).

Before proceeding with the asymptotic analysis at the level of equations we first change the underlying cartesian coordinate system as follows.

3. Conformal mapping. A mapping from a uniform strip onto the fluid domain at rest is constructed analytically. Let the former (computational) domain be defined in the complex w-plane and the rough undisturbed channel (physical domain) be defined in the complex z-plane. Properties of the $z(w)$ mapping will be calculated below. As will be shown working with a symmetric domain is very convenient for the asymptotic analysis to be performed. This is the reason why we solve the (harmonic) conformal mapping problem in such a symmetric configuration (c.f. figure 3.1). Moreover, instead of refering to the w-plane as our computational domain we will (equivalently) interpret our formulation as working with orthogonal curvilinear coordinates in the physical domain (the w-plane horizontal and vertical level curves). In figure 3.1 we superimpose the symmetric domain in the complex z-plane with the curvilinear level curves from the w-plane coordinate system. The polygonal line at the bottom of figure 3.1 is a schematic representation of the topography.

Following Hamilton [6] we define a symmetric flow domain by reflecting the original one about the undisturbed free surface (c.f. figure 3.1). We denote this domain by Ω_z where $z = x + i\sqrt{\beta}y$ and consider it as the conformal image of the strip Ω_w where $w = \xi + i\tilde{\zeta}$ with $|\tilde{\zeta}| \le \sqrt{\beta}$. Then $z = x(\xi,\tilde{\zeta}) + i\sqrt{\beta}y(\xi,\tilde{\zeta}) = x(\xi,\tilde{\zeta}) + i\tilde{y}(\xi,\tilde{\zeta})$ with x and $\tilde{y}$ a pair of harmonic functions on Ω_w. As will become clear in the following sections (in particular section 5) working with x and y is convenient for long wave (shallow water) asymptotics. The depth is kept fixed in this case. On the other hand working with x and $\tilde{y}$ is convenient for computing harmonic functions because the parameter β drops from the Laplacian. These are the reasons why we switch from one scaling to the other.

As will become clear, our main goal is to calculate $\tilde{y}_{\tilde{\zeta}}$ along the undisturbed free surface $\tilde{\zeta} = \tilde{y} = 0$. This coefficient is calculated analytically by solving Laplace's equation for the immaginary part of the conformal change of variables. Once this coefficient is obtained we proceed with the derivation of the full potential theory equations in the curvilinear $(\xi, \tilde{\zeta})$ coordinate system.

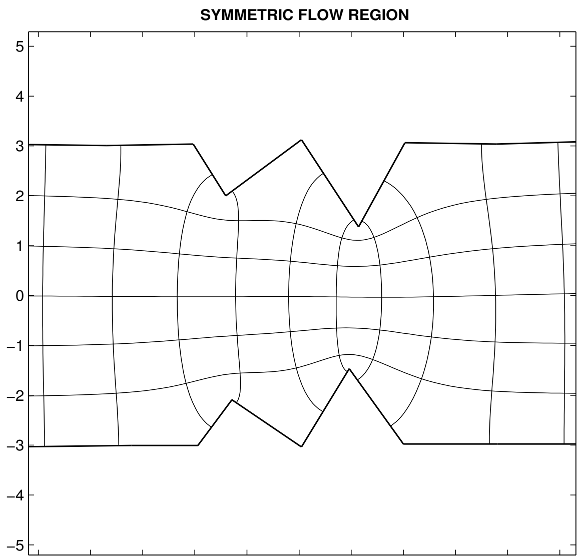

FIG. 3.1. *The symmetric domain in the complex z-plane, where $z = x(\xi, \tilde{\zeta}) + i\tilde{y}(\xi, \tilde{\zeta})$. The lower half ($x \in [-5, 5]$, $y \in [-3, 0]$) is the physical channel with $y = \tilde{\zeta} = 0$ indicating the undisturbed free surface. Superimposed in this complex z-plane domain are the (curvilinear) coordinate level curves from the w-plane system $\xi\tilde{\zeta}$. The polygonal line at the bottom of the figure is a schematic representation of the topography (where $\tilde{\zeta} = \pm\sqrt{\beta}$). This figure was generated using SC-Toolbox [4].*

The immaginary part of the conformal map is the harmonic function that satisfies [6, 11]

$$\Delta\, \tilde{y}(\xi, \tilde{\zeta}) \;=\; 0 \quad \text{in } \Omega_w \tag{3.1}$$

with Dirichlet boundary conditions

$$\tilde{y}(\xi, \pm\sqrt{\beta}) \;=\; \pm\, h(x(\xi)) \equiv \pm\sqrt{\beta} H\left(\frac{x(\xi, \pm\sqrt{\beta})}{\gamma}\right). \tag{3.2}$$

Its harmonic conjugate is $x(\xi, \tilde{\zeta})$. The Green's function for problem (3.1–3.2) is slightly different from Hamilton's because we introduce dimensionless variables and keep depth effects through the parameter $\sqrt{\beta}$. The Green's function, vanishing along the lines $\tilde{\zeta} = \pm\sqrt{\beta}$, is given by

$$G(w; w_0) = \; \mathbf{Re}\; log\; \left((e^{\pi w/2\sqrt{\beta}} \;-\; e^{\pi w_0/2\sqrt{\beta}}) / (e^{\pi w/2\sqrt{\beta}} + e^{\pi \overline{w_0}/2\sqrt{\beta}}) \right) \tag{3.3}$$

where **Re** stands for the real part and the overbar denotes complex conjugation. Near a source point w_0

$$G(w; w_0) \sim \; \mathbf{Re}\; log(w - w_0),$$

meaning that it behaves like the free-space Green's function. At the solid boundaries $\tilde{\zeta} = \pm\sqrt{\beta}$

$$G \equiv 0.$$

Additional asymptotic properties are [6]

$$G, \quad G_\xi \to 0 \quad \text{as} \quad \xi \to \pm\infty \quad \text{in} \quad -\sqrt{\beta} \leq \tilde{\zeta} \leq \sqrt{\beta}.$$

Using Green's third identity we have that

$$2\pi\ \tilde{y}(\xi_0, \tilde{\zeta}_0) \ = \ \oint_{\partial\Omega_w} \ \tilde{y}(\xi, \tilde{\zeta})\ \frac{dG}{dn}(w; w_0)\ ds.$$

By the conditions above this is the same as

$$2\pi\ \tilde{y}(\xi_0, \tilde{\zeta}_0) \ = \ \int_{-\infty}^{\infty} \ h(x(\xi)) \ \left(G_{\tilde{\zeta}}^{+} \ + \ G_{\tilde{\zeta}}^{-}\right)\ d\xi,$$

where

$$G_{\tilde{\zeta}}^{+} = \frac{\partial G}{\partial \tilde{\zeta}}(\xi, +\sqrt{\beta}; \xi_0, \tilde{\zeta}_0) \quad \text{and} \quad G_{\tilde{\zeta}}^{-} = \frac{\partial G}{\partial \tilde{\zeta}}(\xi, -\sqrt{\beta}; \xi_0, \tilde{\zeta}_0).$$

Differentiating this identity with respect $\tilde{\zeta}_0$ and evaluating at $\tilde{\zeta}_0 = 0$ we get our quantity of interest. Namely we have that at the undisturbed free surface

$$\tilde{y}_{\tilde{\zeta}_0}(\xi_0, 0) \ = \ \frac{1}{2\pi} \int_{-\infty}^{\infty} \ h(x(\xi)) \left(G_{\tilde{\zeta}\tilde{\zeta}_0}^{+} \ + \ G_{\tilde{\zeta}\tilde{\zeta}_0}^{-}\right) d\xi. \tag{3.4}$$

The kernel comes from evaluating

$$G_{\tilde{\zeta}\tilde{\zeta}_0}(\xi, -\sqrt{\beta}; \xi_0, 0) \ + \ G_{\tilde{\zeta}\tilde{\zeta}_0}(\xi, \sqrt{\beta}; \xi_0, 0) \ = \ \frac{2\pi^2}{\beta} \ \ \frac{e^{\frac{\pi}{\sqrt{\beta}}(\xi+\xi_0)}}{(e^{\frac{\pi}{\sqrt{\beta}}\xi} + e^{\frac{\pi}{\sqrt{\beta}}\xi_0})^2} \ = \tag{3.5}$$

$$= \ \frac{\pi^2/\beta}{2\ cosh^2 \frac{\pi}{2\sqrt{\beta}}(\xi - \xi_0)}$$

and finally we obtain

$$\tilde{y}_{\tilde{\zeta}_0}(\xi_0, 0) = \ \frac{\pi}{4\beta} \ \int_{-\infty}^{\infty} \ \frac{\sqrt{\beta} H(x(\xi, -\sqrt{\beta})/\gamma)}{cosh^2 \frac{\pi}{2\sqrt{\beta}}(\xi - \xi_0)} d\xi. \tag{3.6}$$

This expression was obtained by Hamilton [6], but without the $\beta^{1/2}$-scaling. This intermediate $\beta^{1/2}$-scale plays an important role indicating the degree of topography smoothing. The rate of smoothing actually depends on $\beta^{1/2}/\gamma$. Numerical examples of the topography smoothing are presented at the end of this paper (figures 6.1 and 6.2). We call $\beta^{1/2}$ an intermediate scale because we will work with an integer power expansion in β as in Whitham's [16] derivation of Boussinesq's equations.

In the $(\xi, \tilde{\zeta})$ coordinate system the varying bottom topography is straightened out and a variable coefficient, namely $\tilde{y}_{\tilde{\zeta}}$ will appear in the free surface condition. Before writing the equations in the $(\xi, \tilde{\zeta})$ system note that

$$(3.7) \qquad \int_{-\infty}^{\infty} \frac{\pi}{4\sqrt{\beta}}\ sech^2\left[\frac{\pi}{2\sqrt{\beta}}(x-y)\right] dx \ = \ \frac{1}{2}\ tanh\left[\frac{\pi}{2\sqrt{\beta}}x\right]_{-\infty}^{\infty} = 1.$$

Hence as $\sqrt{\beta} \downarrow 0$ the kernel in equation (3.6) goes to a delta function and the bottom is felt at the free surface level without any smoothing. Smoothing takes place only for $\beta^{1/2} > 0$.

At the undisturbed level we define the *variable free surface coefficient*

$$M(\xi) \equiv \tilde{y}_{\tilde{\zeta}}(\xi, 0) = 1 + m(\xi)$$

where

$$(3.8) \quad m(\xi; \sqrt{\beta}, \gamma) \equiv \frac{\pi}{4\sqrt{\beta}} \int_{-\infty}^{\infty} \frac{n(x(\xi_0, -\sqrt{\beta})/\gamma)}{cosh^2 \frac{\pi}{2\sqrt{\beta}}(\xi_0 - \xi)} d\xi_0 \ = \ (K * (n \circ x))(\xi).$$

The $(\sqrt{\beta}, \gamma)$ parameter dependence will be omited for brevity. We are ready to rewrite the potential theory equations in the $(\xi, \tilde{\zeta})$ coordinate system. The velocity potential $\phi(\xi, \tilde{\zeta}, t)$ when represented in the curvilinear coordinate system is such that

$$\phi_\xi = \phi_x\ x_\xi(\xi, \tilde{\zeta}) + \phi_{\tilde{y}}\ \tilde{y}_\xi(\xi, \tilde{\zeta})$$

and

$$\phi_{\tilde{\zeta}} = \phi_x\ x_{\tilde{\zeta}}(\xi, \tilde{\zeta}) + \phi_{\tilde{y}}\ \tilde{y}_{\tilde{\zeta}}(\xi, \tilde{\zeta}).$$

In particular at the undisturbed free surface, or for linear problems,

$$\phi_\xi(\xi, 0) = M(\xi)\phi_x$$

and

$$\phi_{\tilde{\zeta}}(\xi, 0) = M(\xi)\phi_{\tilde{y}}.$$

Note that we have used the Cauchy–Riemann equations. Inverting the relation given above we have

$$(3.9) \qquad \phi_x = \frac{1}{|J|}\left[\tilde{y}_{\tilde{\zeta}}\phi_\xi - \tilde{y}_\xi\phi_{\tilde{\zeta}}\right]$$

and

$$(3.10) \qquad \phi_{\tilde{y}} = \frac{1}{|J|}\left[-x_{\tilde{\zeta}}\phi_\xi + x_\xi\phi_{\tilde{\zeta}}\right],$$

where

$$|J| = x_\xi\tilde{y}_{\tilde{\zeta}} - \tilde{y}_\xi x_{\tilde{\zeta}} = \tilde{y}_{\tilde{\zeta}}^2 + \tilde{y}_\xi^2.$$

Moreover

$$(3.11) \qquad \phi_x^2 + \phi_{\tilde{y}}^2 = \frac{1}{|J|}\left(\phi_\xi^2 + \phi_{\tilde{\zeta}}^2\right),$$

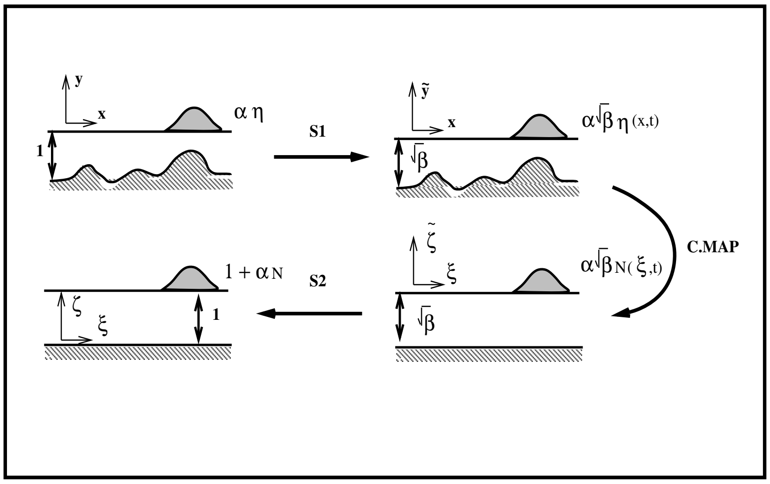

FIG. 3.2. *This is a schematic figure showing the changes of scales performed, indicated by S1, S2 and the Conformal Transformation. The geometries in the left are in the shallow water framework (with unit depth). The geometries in the right are used so that the velocity potential solves Laplace's equation in the corresponding variables.*

which relates the speeds in the two coordinate systems.

In the new coordinate system the position of the free surface will be described by some function, here denoted by $N(\xi, t)$, such that

$$\tilde{\zeta} = \alpha\sqrt{\beta}N(\xi, t). \tag{3.12}$$

The new free surface profile, represented by $N(\xi, t)$, does not necessarily resemble $\eta(x, t)$ as indicated in the schematic figure 3.2. Nevertheless this is a material curve. In the cartesian coordinates $(x, \tilde{y})$ the dimensionless kinematic condition was given by

$$\sqrt{\beta}\eta_t + \alpha\phi_x\sqrt{\beta}\eta_x - \phi_{\tilde{y}} = 0,$$

which is the same as

$$\frac{D}{Dt}\left(\tilde{y} - \alpha\sqrt{\beta}\eta(x, t)\right) = 0,$$

with the convective derivative

$$\frac{D}{Dt} \equiv \partial_t + \alpha\left(\phi_x\partial_x + \phi_{\tilde{y}}\partial_{\tilde{y}}\right).$$

In the curvilinear coordinates it becomes

$$\frac{\mathcal{D}}{\mathcal{D}t} \equiv \partial_t + \frac{\alpha}{|J|}\left(\phi_\xi\partial_\xi + \phi_{\tilde{\zeta}}\partial_{\tilde{\zeta}}\right),$$

where we have used that $\partial_x = |J|^{-1}(\tilde{y}_{\tilde{\zeta}}\partial_\xi - \tilde{y}_\xi\partial_{\tilde{\zeta}})$ and the corresponding expression for $\partial_{\tilde{y}}$ (c.f. equations (3.9) and (3.10)). The new kinematic condition is obtained by performing

$$\frac{\mathcal{D}}{\mathcal{D}t}\left(\tilde{\zeta} - \alpha\sqrt{\beta}N(\xi, t)\right) = 0,$$

and is presented below.

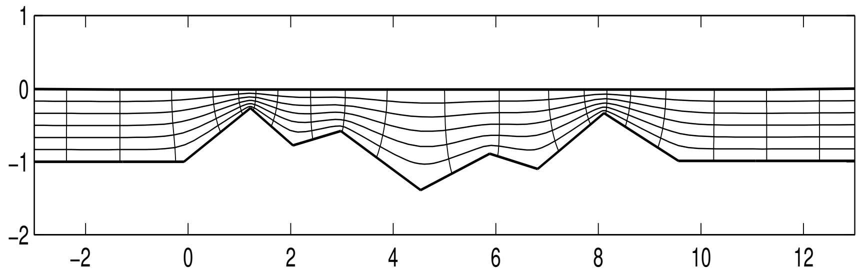

FIG. 4.1. *A schematic figure showing a slowly varying topography in the xy coordinate system together with the ξ and $\tilde{\zeta}$ level curves. This figure was generated using SC-Toolbox [4].*

4. Nonlinear potential theory equations in terrain-following coordinates. The scaled water wave equations in the fixed orthogonal curvilinear coordinates $(\xi, \tilde{\zeta})$ (cf. figure 4.1) are:

$$\phi_{\xi\xi} \;+\; \phi_{\tilde{\zeta}\tilde{\zeta}} \;=\; 0 \qquad -\sqrt{\beta} < \tilde{\zeta} < \alpha\sqrt{\beta}N(\xi, t) \tag{4.1}$$

with free surface conditions

$$|J|N_t + \alpha\phi_\xi N_\xi - \frac{1}{\sqrt{\beta}}\phi_{\tilde{\zeta}} = 0 \tag{4.2}$$

and

$$\phi_t + \eta + \frac{\alpha}{2|J|}\left(\phi_\xi^2 + \phi_{\tilde{\zeta}}^2\right) = 0 \tag{4.3}$$

at $\tilde{\zeta} = \alpha\sqrt{\beta}N(\xi, t)$. The bottom condition is

$$\phi_{\tilde{\zeta}} = 0 \quad \text{ at } \; \tilde{\zeta} = -\sqrt{\beta}. \tag{4.4}$$

Regarding the initial conditions note that by starting with a pulse over a region of uniform depth, the initial data are not affected by the conformal mapping (c.f. figure 4.1 at $x \leq -1$ and $x \geq 11$). We only need to replace x by ξ in the initial wave conditions. Away from the rough region

$$1 + m(\xi) = \tilde{y}_{\tilde{\zeta}}(\xi, 0) \approx 1,$$

where this adjustment is exponentially fast. Numerical evidence of this adjustment is presented in figures 6.1 and 6.2. The exponential adjustment rate depends on $\beta^{1/2}$, the important scale we retained in the coefficient (3.8). Hence from the Cauchy-Riemann equations $x_\xi(\xi, 0) \approx 1$. This was not noticed in Hamilton's work [6] because the analysis was not done in dimensionless variables. Scales were used only to argue which terms could be dropped.

Moreover it is important to point out that these equations are the same as those obtained by Hamilton [6], using a variational principle. The difference is in our use of dimensionless variables. The corresponding dimensionless variational principle is given below for completeness. Hamilton ([6] Appendix A) showed that the $(\xi, \tilde{\zeta})$

change of variables can be used within the functional given in the books of Whitham [16] and Mei [7]. The variational pressure-principle is

$$I = \int \int_{\mathbf{R}} \mathcal{L} dx dt, \tag{4.5}$$

where $\mathbf{R}$ is a region in (x,t) space and the dimensionless Lagrangian is given by

$$\mathcal{L} = -\sqrt{\beta} \int_{-\sqrt{\beta}h(x,y)}^{\alpha\sqrt{\beta}\eta(x,t)} \left[\phi_t + \tilde{y} + \frac{\alpha}{2} (\nabla\phi \cdot \nabla\phi) \right] d\tilde{y}. \tag{4.6}$$

Under the change of variables the functional becomes

$$I = -\sqrt{\beta} \int \int_{\mathbf{R}} \int_{-\sqrt{\beta}}^{\alpha\sqrt{\beta}N} \left[|J| \left(\phi_t + \frac{1}{\sqrt{\beta}} \tilde{y}(\xi, \tilde{\zeta}) \right) + \frac{\alpha}{2} (\nabla\phi \cdot \nabla\phi) \right] d\tilde{\zeta} d\xi dt, \tag{4.7}$$

where now $\nabla = (\partial_\xi, \partial_{\tilde{\zeta}})$. Minimizing this functional, by taking variations in ϕ and N, Hamilton obtained a system of equations similar to the dimensionless one derived above.

5. Asymptotic theory. The asymptotic theory is performed at the level of equations. We are interested in the shallow water/long wave regime. More specifically in the weakly dispersive, weakly nonlinear regime. As mentioned in section 3 it is convenient to normalize in the vertical direction and work with a unit depth channel (c.f. scaling S2, figure 3.2) when performing a long wave (shallow water) asymptotic analysis. The geometry is kept fixed and we can focus on the leading order terms of the asymptotic expansion. Let the origin of the curvilinear coordinate sytem be at the bottom and define $\tilde{\zeta} = \sqrt{\beta}(\zeta - 1)$. Substitute in the equations above to get

$$\beta\phi_{\xi\xi} + \phi_{\zeta\zeta} = 0, \qquad \text{at } 0 < \zeta < 1 + \alpha N(\xi, t), \tag{5.1}$$

with free surface conditions

$$|J| N_t + \alpha\phi_\xi N_\xi - \frac{1}{\beta}\phi_\zeta = 0 \tag{5.2}$$

$$\eta + \phi_t + \frac{\alpha}{2|J|} \left(\phi_\xi^2 + \frac{1}{\beta}\phi_\zeta^2 \right) = 0 \tag{5.3}$$

at $\zeta = 1 + \alpha N(\xi, t)$ and

$$\phi_\zeta = 0 \qquad \text{at } \zeta = 0. \tag{5.4}$$

As in Whitham [16] consider a power series expansion near the bottom of the channel in the form

$$\phi(\xi, \zeta, t) = \sum_{n=0}^{\infty} \zeta^n \, f_n(\xi, t). \tag{5.5}$$

This function satisfies the scaled Laplace equation when

$$f_{m+2} = \frac{-\beta}{(m+2)(m+1)} \frac{\partial^2 f_m}{\partial \xi^2}.$$

Morevover the Neumann condition at the bottom is satisfied when all odd terms (i.e. f_{2m+1}) are zero. Hence by denoting $f_0(\xi,t)=f(\xi,t)$ for simplicity, we have

$$\phi(\xi,\zeta,t)=\sum_{n=0}^{\infty}\frac{(-\beta)^n}{(2n)!}\zeta^{2n}\frac{\partial^{2n}f(\xi,t)}{\partial\xi^{2n}} \tag{5.6}$$

a power series expansion in β. For this reason the $\beta^{1/2}$-scale was called an intermediate scale earlier. The velocity potential, represented by the power series above, satisfies the scaled Laplace equation and the homogeneous Neumann condition along the bottom. Up to this point we have done exactly the same steps as in Whitham's book [16] for a flat channel in cartesian coordinates.

We must now satisfy the free surface conditions. At $\zeta=\zeta_{FS}\equiv 1+\alpha N(\xi,t)$ we have that

$$\phi_\xi(\xi,\zeta_{FS},t)=f_\xi-\frac{\beta}{2}(1+\alpha N)^2 f_{\xi\xi\xi}+O(\beta^2) \tag{5.7}$$

$$\phi_\zeta(\xi,\zeta_{FS},t)=-\beta(1+\alpha N)f_{\xi\xi}+\frac{\beta^2}{3!}(1+\alpha N)^3 f_{\xi\xi\xi\xi}+O(\beta^3) \tag{5.8}$$

and

$$\phi_t(\xi,\zeta_{FS},t)=f_t-\frac{\beta}{2}(1+\alpha N)^2 f_{\xi\xi t}+O(\beta^2). \tag{5.9}$$

Note that both (new) free surface conditions have a time dependent coefficient. This is due to the presence of the Jacobian, of the time independent change of coordinates, evaluated at the time dependent free surface. Within the weakly nonlinear, weakly dispersive approximation considered, it is possible to eliminate this time dependence as will be shown below. Time independent coefficients are better for analysis and computations. As a first step, in this direction, it is worth noticing that at the smooth free surface $\tilde{\zeta}_{FS}=\alpha\sqrt{\beta}N(\xi,t)$ the Jacobian is

$$|J|(\xi,t)=\tilde{y}_\xi^2(\xi,\tilde{\zeta}_{FS})+\tilde{y}_{\tilde{\zeta}}^2(\xi,\tilde{\zeta}_{FS})$$

and by the Taylor polynomial formula

$$|J|(\xi,t)=\tilde{y}_{\tilde{\zeta}}^2(\xi,0)+\alpha^2 R_J(\xi,\tilde{\zeta}_M)=M(\xi)^2+O(\alpha^2),\quad 0<|\tilde{\zeta}_M|<|\tilde{\zeta}_{FS}|. \tag{5.10}$$

The Jacobian can be well approximated by an $O(1)$ time independent coefficient. The time dependent correction term is $O(\alpha^2)$ due to the fact that the curvilinear coordinate system is symmetric about $\tilde{y}=\tilde{\zeta}=0$. There are no $O(\alpha)$ terms. For the same reason, approximating $\tilde{\zeta}(x,\tilde{y}_{FS})$ in $\tilde{y}$ leads to

$$N(\xi,t)=\frac{1}{M(\xi)}\eta(x(\xi),t)+\alpha^2\beta R_N(\xi,\tilde{y}_M),\quad 0<|\tilde{y}_M|<|\tilde{y}_{FS}|. \tag{5.11}$$

Substituting expressions (5.7)-(5.11) in the free surface conditions we get

$$\eta+f_t-\frac{\beta}{2}f_{\xi\xi t}+\frac{\alpha}{2M^2(\xi)}f_\xi^2=O(\alpha\beta,\beta^2)$$

$$M(\xi)\,\eta_t + \left[\left(1 + \frac{\alpha}{M(\xi)}\eta\right) f_\xi\right]_\xi - \frac{\beta}{6} f_{\xi\xi\xi\xi} = O(\alpha^2, \alpha\beta, \beta^2).$$

The variable coefficients are time independent and depend only on $\tilde{y}_{\zeta}(\xi, 0)$ as mentioned before in the conformal mapping section.

As in Whitham [16] it is useful to work with a conveniently averaged velocity component. From equation (5.7) we have that

$$\phi_\xi(\xi, \zeta_{FS}, t) \equiv u(\xi, \zeta_{FS}, t) = \tilde{u}(\xi, t) - \frac{\beta}{2}\zeta_{FS}^2 \tilde{u}_{\xi\xi}(\xi, t) + O(\beta^2),$$

where $\tilde{u} \equiv f_\xi$ is the "slip–velocity" along the bottom topography. In analogy with the σ–coordinates used in atmospheric flows [5], we call ϕ_ξ the terrain–following velocity component [3]. Its transversal average (along a ξ level-curve) is defined as

$$U(\xi, t) \equiv \frac{1}{\zeta_{FS}} \int_0^{\zeta_{FS}} \phi_\xi(\xi, \zeta, t)\, d\zeta. \tag{5.12}$$

In physical space this integral represents a weighted average of the terrain-following velocity components. We provide further insight about the averaging in figure 5.1. Therefore using the potential's power series representation

$$U(\xi, t) = \sum_{n=0}^{\infty} \frac{(-\beta)^n}{(2n)!} \left[\frac{1}{\zeta_{FS}} \int_0^{\zeta_{FS}} \zeta^{2n} d\zeta\right] \frac{\partial^{2n+1} f(\xi, t)}{\partial \xi^{2n+1}} = \tilde{u} - \frac{\beta}{6}\tilde{u}_{\xi\xi} + O(\alpha\beta, \beta^2).$$

Differentiate the first free surface condition with respect to ξ and substitute for depth–averaged velocity through the expansion

$$\tilde{u} = U + \frac{\beta}{6} U_{\xi\xi} + O(\alpha\beta, \beta^2).$$

We get a **terrain-following Boussinesq system**

$$\begin{cases} M(\xi)\eta_t + \left[(1 + \alpha\eta/M(\xi))\, U\right]_\xi = 0 \\ U_t + \eta_\xi + \frac{\alpha}{2}\left[U^2/M^2(\xi)\right]_\xi - \frac{\beta}{3} U_{\xi\xi t} = 0. \end{cases} \tag{5.13}$$

This is a weakly nonlinear, weakly dispersive system with variable coefficients, all depending on $M(\xi; \sqrt{\beta}, \gamma)$. The $O(\alpha^2, \alpha\beta, \beta^2)$ truncation terms are small and were dropped. This was not the case when working with a cartesian coordinate system. The truncation terms could be large. Note that working with the terrain-following velocity we generated (formally) a converging asymptotic expansion. This is true even in the presence of rapidly varying topographies ($\gamma \ll 1$), as opposed to the original (nonconverging) expansion in cartesian coordinates. Our physical interpretation is that the Boussinesq system with weighted terrain-following velocities averages is more representative, as an asymptotic simplification of the full set of equations. Namely, the bulk of the terrain-following velocity components do not deviate too much from their average as opposed to the horizontal components. Figure 5.1 corroborates with this interpretation from a graphical perspective. The weighted velocity averages are performed over the ξ level-curves (vertical curves in figure 5.1; curves over which ζ varies, but ξ is fixed). Note that even with high graphing resolution (figure 5.1(B)) the effective flow domain penetrates very little into the narrow valleys. The bulk of the

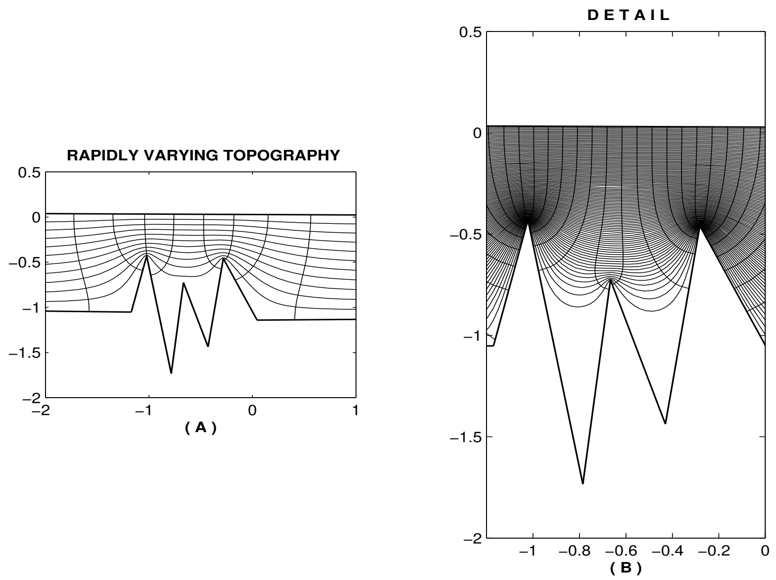

FIG. 5.1. *The effective flow domain. The horizontal resolution is equal to (A) 10 ζ level-curves. (B) 100 ζ level-curves. This figure was generated using SC-Toolbox [4].*

average is performed over the smoothly varying "outer" terrain-following velocities. In other words the contribution from the highly corrugated valleys is very small: 10% below the lowest ζ level-curve in 5.1(A) and 1% in 5.1(B). Clearly the outer flow prevails in the weighted average (5.12). In contrast if the topography is slowly varying the weights for the inner valley regions will be larger as indicated in figure 4.1.

Regarding the use of averaged velocities, we do this change of dependent variables because standard long wave models use depth averaged velocities. Moreover, the use of this dependent variable improves the stability for the high wavenumber regime of the Boussinesq system.

When the channel is flat the **metric term** ($M(\xi) = 1 + m(\xi)$) reduces to one and we recover the standard dimensionless Boussinesq system [16]. Note that system (5.13) is different from that obtained by Hamilton (c.f. equations (A14) and (A15) in [6]), which has powers of the metric term and an η_{tt} term. A comparison with standard Boussinesq systems is presented in the appendix of the present paper. When linearized they all have the same dispersion relation.

6. Applications and conclusions. We now point out some important features regarding applications with the terrain-following Boussinesq system:

(i) The derivatives of the topography–related coefficients are all well defined, even in the presence of corners or steps along the bottom. The metric term $M(\xi)$ is an analytic function. This is not the case in the classical Boussinesq equations (c.f. Appendix A) as pointed out in Hamilton's work [6].

(ii) Under the curvilinear coordinate formulation, the **nonlinear shallow water equations** are viewed as an $O(\alpha, \sqrt{\beta})$ approximation to the full potential theory equations. Dropping the $O(\beta)$ term from system (5.13) above, we are left with a hyperbolic system, but we are still keeping an $O(\sqrt{\beta})$ term inside the metric term

(c.f. (3.8)):

$$
\left\{
\begin{array}{l}
M(\xi;\sqrt{\beta},\gamma)\eta_t + \left[\left(1+\alpha\eta/M(\xi;\sqrt{\beta},\gamma)\right)U\right]_\xi = 0 \\
\\
U_t + \eta_\xi + \frac{\alpha}{2}\left[U^2/M^2(\xi;\sqrt{\beta},\gamma)\right]_\xi = 0.
\end{array}
\right. \tag{6.1}
$$

This has a great advantage in opposition to the $\beta \to 0$ limit used in the standard shallow water derivations. In the limiting $\beta \to 0$ case derivatives at corners along the bottom are not defined. In the present formulation consistency is preserved between the two formulations since in the vanishing β limit the kernel of the metric term goes to a Dirac delta function (c.f. equation (3.7)) and singularities at the bottom are recovered. But retaining the intermediate $O(\sqrt{\beta})$ term leads to a (hyperbolic) shallow water system having a smooth, well defined coefficient. Even if the topography has corners. The degree of smoothing/averaging performed by the metric–kernel is controlled by $\sqrt{\beta}$ and γ (c.f. equation (3.8)). This last point was not observed in Hamilton's work [6] since the metric term was not scaled in terms of depth/wavelength scales. By averaging we mean cases where the bottom is rapidly varying ($\gamma \ll 1$).

A schematic example is presented in figure 6.1. The conformal mapping was computed numerically [12] as well as the metric term. We considered periodic mountain ranges having identical triangular mountains. The height of each triangle is equal to 0.5 and the base equal to 2.0 units. A natural question to ask is what is the underlying value of β in this example? As will be discussed below, the averaging effect is related to the ratio between the scales $\sqrt{\beta}$ and γ. This was pointed out in Nachbin [12] (page 366) where a rule was devised in order to incorporate both scales. In order to incorporate these two scales the Schwarz-Christoffel mapping was performed on mountains varying on the "modified" length scale

$$\tilde{l}_b \equiv l_b/(\sigma\sqrt{\beta}).$$

Note the difference of notations from [12]: $l_p \equiv \sigma$ and ($\beta = h_0/\lambda$) there is the $\sqrt{\beta}$ here. In other words

$$\sqrt{\beta} = \gamma/\tilde{l}_b.$$

Since for the triangular mountains $\tilde{l}_b = 2$, then we have that $\beta = 0.25\gamma^2$. A typical γ for rapidly varying topograhies is 0.1 (10 mountain peaks per pulse width).

In the first example we contrast the metric term for a periodic mountain range with 5 mountains with that for a mountain range (of the same period) with 7 mountains. We clearly observe the exponential adjustment mentioned earlier. We also observe the smoothing along the sharp summit of the triangular mountains and the averaging as we put the mountains closer together (c.f. figure 6.2). In this case we have $\tilde{l}_b = 1$ and therefore $\beta = \gamma^2$. As indicated above averaging (in a homogenization sense) takes place as soon as the mountain scale parameter γ is smaller than the support of the $sech^2$–kernel, controlled by $\beta^{1/2}$ (equation (3.7)). Note that the topography's derivative scales like $1/\gamma$ while the metric term's derivative always scales like $1/\sqrt{\beta}$. One of the advantages of this formulation is that the latter is independent of γ. This is a useful fact in the discussion that follows.

(iii) It is worth pointing out that first order derivatives of the metric term are produced. These terms are $O(1/\sqrt{\beta})$ (c.f. equation (3.8)) and are generated by the N_ξ term, in the kinematic condition, and by differentiating Bernoulli's Law with respect to ξ. In particular these $O(1/\sqrt{\beta})$ terms are present in the $O(\alpha\beta, \beta^2)$ terms that were

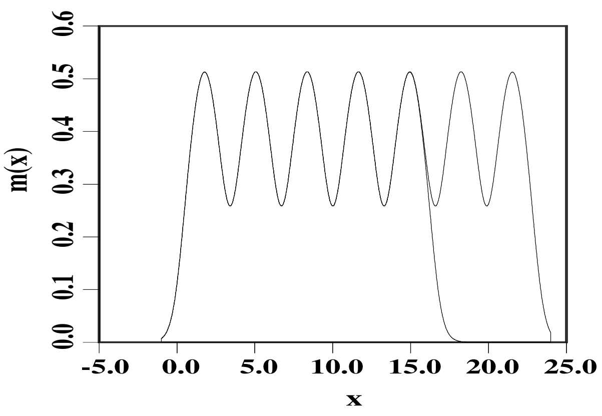

FIG. 6.1. *The metric term $m(\xi) = M(\xi) - 1$ for two periodic topographies. One was generated by 5 triangular mountains along the bottom while the other by 7 triangular mountains. The two metric terms match very well over the first 5 mountains, confirming the exponentially fast adjustment mentioned earlier. The $\beta^{1/2}$ scale plays a role in this adjustment.*

dropped from Bernoulli's Law. Nevertheless one should not be concerned with the loss of validity of the asymptotics. The $O(1/\sqrt{\beta})$ term does not alter the ordering of the terms presented in the asymptotic analysis above. It can be easily verified that when equation

$$\eta + f_t - \frac{\beta}{2} f_{\xi\xi t} + \frac{\alpha}{2M^2(\xi)} f_\xi^2 = O(\alpha\beta, \beta^2)$$

is differentiated with respect to ξ, the $1/\sqrt{\beta}$ term will only affect the $O(\alpha\beta)$ terms. For example if we take the $O(\alpha\beta)/\sqrt{\beta}$ and compare it to the leading $O(\alpha)$ nonlinearity term we easily note that reordering takes place only if $\sqrt{\beta} > 1$ which is not the long wave regime we started with. Hence as long as $0 < \beta \ll 1$ the equations derived are valid weakly nonlinear, weakly dispersive approximations to the nonlinear potential theory equations. Namely they are valid as the leading order corrections in α and in β. The question of including the next order terms (in either parameter) was not relevant to our application of interest [9]. Perhaps there are applications where these terms might play a role. We have not attempted to identify these regimes. Having set that $\beta > 0$ guarantees that the variable coefficients can be differentiated in the standard way. Delta functions do not arise at discontinuities of the topography.

(iv) Regarding applications these new equations enable the study of the interaction of linear and nonlinear long surface waves with rapidly varying features of the topography. To our knowledge up to the present date only small amplitude or mild slope topographies have been considered for Boussinesq type models. The present model expands the regime of applicability and is consistent with previous cartesian

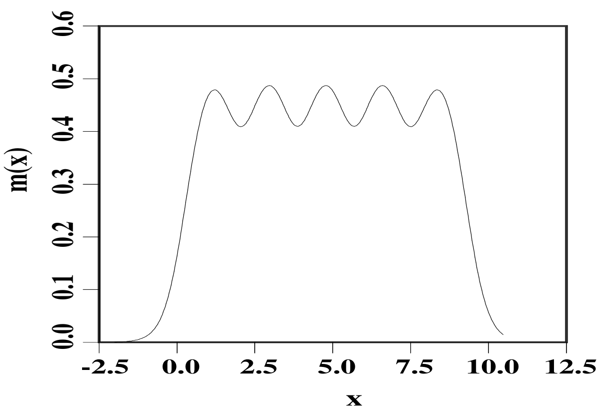

FIG. 6.2. *Averaging observed through the metric term $m(\xi) = M(\xi) - 1$. The triangular mountains are closer together, i.e. varying on a faster scale. The base of each triangle is 1/2 of those in figure 6.1.*

formulations in the case where $\gamma \gg 1$. In this regime the conformal mapping is nearly the identity map at the free surface level.

Many new theoretical and numerical problems can now be addressed with this new curvilinear formulation. A particular theoretical problem that we investigated through this new model is the O'Doherty-Anstey approximation of weakly dispersive waves. This theory characterizes the apparent diffusion of transmitted pulses due to disordered multiple scattering. This theory, initially developed for acoustic waves [1], was generalized to weakly dispersive waves by Muñoz Grajales and Nachbin [9]. Using the terrain-following Boussinesq system we obtained expressions that capture both the attenuation of the transmitted pulse as well as the forward scattering radiation. Numerical validation experiments include the apparent diffusion of solitary waves in the presence of a highly disordered topography. We are currently also investigating an interesting numerical problem regarding the use of the terrain-following formulation [10]. The classical system (A.2) contains a term difficult to handle numerically in the presence of a topography. This is because the topography–related coefficients multiply the terms with higher order derivatives. In the curvilinear formulation the higher order term has a constant coefficient. We have obtained numerical evidence [10] that the "repositioning" of topography related terms (namely the metric terms) leads to improvements in the performance of Boussinesq solvers. We have also obtained results regarding the time reversed refocussing (i.e. waveform inversion) for weakly dispersive waves [10].

The Boussinesq system (5.13) can be cast into a second order differential equation.

Take the system at the stage where we had

$$\eta + f_t - \frac{\beta}{2} f_{\xi\xi t} + \frac{\alpha}{2M^2(\xi)} f_\xi^2 = O(\alpha^2, \alpha\beta, \beta^2)$$

$$M(\xi)\ \eta_t + \left[\left(1 + \frac{\alpha}{M(\xi)}\eta\right) f_\xi\right]_\xi - \frac{\beta}{6} f_{\xi\xi\xi\xi} = O(\alpha^2, \alpha\beta, \beta^2).$$

From these equations we have that

$$\eta_t = -f_{tt} + O(\alpha, \beta), \quad M(\xi)\eta_t = -f_{\xi\xi} + O(\alpha, \beta) \ \text{ and } \ f_{\xi\xi} = M(\xi) f_{tt} + O(\alpha, \beta).$$

These approximations are used after we calculate the time derivative of the first equation, multiply it by $M(\xi)$ and subtract it from the second equation to get

$$f_{\xi\xi} - M f_{tt} + \frac{\beta}{3} M f_{\xi\xi tt} - \frac{\alpha}{M}\left[f_\xi^2 + \frac{M}{2} f_t^2\right]_t + \alpha\left(\frac{M'}{M^2}\right) f_t f_\xi = O(\alpha^2, \alpha\beta, \beta^2). \tag{6.2}$$

By dropping the $O(\alpha^2, \alpha\beta, \beta^2)$ term we get the second order Boussinesq equation governing the velocity potential along the bottom topography. It is interesting to note that in the Boussinesq system (5.13) no new terms were generated by the curvilinear coordinates. The only novelty is the presence of the metric term $M(\xi)$. Nevertheless a new term appears, when the system is reduced to a second order differential equation. The new term contains the derivative of the metric term. Again, in the absence of a topography, this differential equation reduces to the standard second order Boussinesq equation [7].

Appendix A. Boussinesq models and their linearization.

Consider Peregrine's model (Mei [7] page 512):

$$\eta_t + \nabla \cdot [(h + \eta)U] = 0 \tag{A.1}$$

$$U_t + U \cdot \nabla U + g\nabla\eta = \frac{h}{2}\nabla\left[\nabla \cdot (hU_t)\right] - \frac{h^2}{6}\nabla\left[\nabla \cdot U_t\right].$$

Restricting to one-dimensional flows it becomes

$$\eta_t + \partial_x\left[(h + \eta)U\right] = 0 \tag{A.2}$$

$$U_t + UU_x + g\eta_x = \frac{h}{2}\left[\partial_x^2(hU_t)\right] - \frac{h^2}{6} U_{xxt}.$$

Linearize this system by letting $\tilde{\eta} = \varepsilon\eta$ and $\tilde{U} = \varepsilon U$. Drop the $\tilde{}$ to get

$$\eta_t + (hU)_x = 0 \tag{A.3}$$

$$U_t + g\eta_x = \frac{h}{2}(hU_t)_{xx} - \frac{h^2}{6} U_{xxt}.$$

Moreover, if the bottom is flat $(h(x) \equiv h_0)$

$$\eta_t + h_0 U_x = 0 \tag{A.4}$$

$$U_t + g\eta_x = \frac{h_0^2}{3} U_{xxt}.$$

The dimensionless Boussinesq equation derived in Whitham (page 467; using the dispersion relation) is

$$\eta_t + U_x = 0 \tag{A.5}$$

$$U_t + \eta_x = -\frac{\beta}{3}\eta_{xtt}.$$

Moreover the linearized terrain-following Boussinesq equation is

$$M(\xi)\eta_t + U_\xi = 0 \tag{A.6}$$

$$U_t + \eta_\xi = \frac{\beta}{3} U_{\xi\xi t}.$$

All these Boussinesq systems share **the same dispersion relation**:

$$\omega^2 = \frac{k^2}{1 + \frac{1}{3}\beta k^2}, \tag{A.7}$$

which is stable as $k \to \infty$. In equation (A.4) the variables are in their original dimensions. Thus, for the sake of comparison, we set $gh_0 = 1$ and $h_0^2 = \beta$. This means that the characteristic wavelength is taken to be equal to one.

REFERENCES

[1] R.Burridge, and L. Berlyand, The accuracy of the O'Doherty-Anstey approximation for wave propagating in highly disordered stratified media, Wave Motion, **21** (1995), pp. 357-373.

[2] R. Camassa, D.D. Holm, and C.D. Levermore,, Long–Time shallow–water equations with a variable bottom, J. Fluid Mech., **vol. 349** (1997), pp. 173–189.

[3] T.L. Clark, A small scale dynamical model using a terrain–following coordinate transformation, J. Comput. Phys., **24** (1977), pp. 136–215.

[4] T. Driscoll, http://www.math.udel.edu/ driscoll/software.

[5] A.E. Gill, *Atmosphere–Ocean Dynamics*, Academic Press, 1982.

[6] J. Hamilton, Differential equations for long-period gravity waves on a fluid of rapidly varying depth, J. Fluid Mech., **vol. 83** (1977), pp. 289–310.

[7] C.C. Mei, *The Applied Dynamics of Ocean Surface Waves*, John Wiley, 1983.

[8] P. Milewski, Long wave interaction over varying topography, Physica D, 123 (1998), pp. 36–47.

[9] J.C. Muñoz Grajales and A. Nachbin, Dispersive wave attenuation due to orographic forcing, submitted for publication, 2002.

[10] J.C. Muñoz Grajales and A. Nachbin, Dispersive pulse stabilization and solitary wave refocusing, in preparation, 2002.

[11] A. Nachbin, *Modelling of Water Waves in Shallow Channels*, Computational Mechanics Publications, Southampton, U.K., 1993.

[12] A. Nachbin, The localization length of randomly scattered water waves, J. Fluid Mech., **Vol. 296** (1995), pp. 353–372.

[13] A. Nachbin and G.C. Papanicolaou, Water waves in shallow channels of rapidly varying depth, J. Fluid Mech., **Vol. 241** (1992), pp. 311–332.

[14] R.R. Rosales and G.C. Papanicolaou, Gravity waves in a channel with a rough bottom, Studies in Appl. Math., **68** (1983), pp. 89–102.

[15] H.A. Schäffer and P.A. Madsen, *Further enhancements of Boussinesq-type equations*, Coastal Eng., 26 (1995), pp. 1–14.

[16] G.B. Whitham, *Linear and Nonlinear Waves*, John Wiley, 1974.